Neurectomy preserves fast fibers when combined with tenotomy of infraspinatus muscle via upregulation of myogenesis

Flück, Martin ; Valdivieso, Paola ; Ruoss, Severin ; von Rechenberg, Brigitte ; Benn, Mario C ; Meyer, Dominik C ; Wieser, Karl ; Gerber, Christian

Abstract: INTRODUCTION We evaluated the contribution of denervation-related molecular processes to rotator cuff muscle degeneration after tendon release. METHODS We assessed the levels of myogenic (myogenin and myogenic differentiation factor [myoD]) and pro-adipogenic (peroxisome proliferator-activated receptor gamma) transcription factors; the denervation-associated proteins tenascin-C, laminin-2, and calcium/calmodulin dependent kinase II (CaMKII); and cellular alterations in sheep after infraspinatus tenotomy (TEN), suprascapular neurectomy (NEU), or both (TEN-NEU). RESULTS Extracellular ground substance increased at the expense of contractile tissue 16 weeks after surgery, correlating with CaMKII isoform levels. Sheep undergoing NEU and TEN-NEU had exaggerated infraspinatus atrophy and increased fast fibers compared with TEN sheep. The MCaMKII isoform levels increased with tenotomy, and myoD levels tripled after denervation and were associated with slow fibers. DISCUSSION In sheep, denervation did not affect muscle-to-fat conversion after tenotomy of the infraspinatus. Furthermore, concurrent neurectomy mitigated the loss of fast fibers after tenotomy by inducing a fast-contractile phenotype.

DOI: https://doi.org/10.1002/mus.26316

Neurectomy preserves fast fibers when combined with tenotomy of infraspinatus muscle via upregulation of myogenesis

Running title: Protein expression with denervation and tenotomy

Martin Flück, PhD1¶; Paola Valdivieso, PhD1; Severin Ruoss PhD1; Brigitte von Rechenberg, DVM ECVS2; Mario C Benn, DVM2; Dominik C Meyer, MD3; Karl Wieser, MD3; Christian Gerber, MD FRCS3

1Laboratory for Muscle Plasticity, Department of Orthopedics, University of Zurich; 2 Musculoskeletal Research Unit, Department of Molecular Mechanisms, Vetsuisse Faculty, University of Zurich; 3Department of Orthopedics, Balgrist University Hospital, University of Zurich

¶ corresponding author
Laboratory for Muscle Plasticity
Department of Orthopedics, University of Zurich
Balgrist Campus, Lengghalde 5
8008 Zurich, Switzerland
Tel: +41 44 386 7350
email: martin.flueck@balgrist.ch

No conflict

Funding: Support was received from the RESORTHO Foundation and grants 3200 B_127086 and 310030_149786 from the Swiss National Science Foundation.

Ethics: We confirm that we have read the Journal's position on issues involved in ethical publication and affirm that this report is consistent with those guidelines

This article has been accepted for publication and undergone full peer review but has not been through the copyediting, typesetting, pagination and proofreading process, which may lead to differences between this version and the Version of Record. Please cite this article as doi: 10.1002/mus.26316

Abstract

Introduction: We evaluated the contribution of denervation-related molecular processes to rotator cuff muscle degeneration after tendon release.

Methods: We assessed the levels of myogenic (myogenin and myogenic differentiation factor [myoD]) and pro-adipogenic (peroxisome proliferator-activated receptor gamma) transcription factors; the denervation-associated proteins tenascin-C, laminin-2, and calcium/calmodulin dependent kinase II (CaMKII); and cellular alterations in sheep after infraspinatus tenotomy (TEN), suprascapular neurectomy (NEU), or both (TEN-NEU).

Results: Extracellular ground substance increased at the expense of contractile tissue 16 weeks after surgery, correlating with CaMKII isoform levels. Sheep undergoing NEU and TEN-NEU had exaggerated infraspinatus atrophy and increased fast fibers compared with TEN sheep. The βMCaMKII isoform levels increased with tenotomy, and myoD levels tripled after denervation and were associated with slow fibers.

Discussion: In sheep, denervation did not affect muscle-to-fat conversion after tenotomy of the infraspinatus. Furthermore, concurrent neurectomy mitigated the loss of fast fibers after tenotomy by inducing a fast-contractile phenotype.

Keywords: fatty infiltration, nerve, tenotomy, regeneration, transcription factor, calcium

Introduction

Full or partial tears of rotator cuff tendons occur relatively frequently, affecting 2 in 5 persons over 60 years of age [1]. Consequently, some functions of the upper extremities, specifically the hand, may be severely deteriorated [2]. Untreated full-thickness tendon tears lead to degeneration of the released muscle through the loss of muscle fibers/contractile material and a relative increase in fat cells [3,4], which may irreversibly affect shoulder function. Increased fat content in rotator cuff muscle after tendon release is associated with an altered fiber type distribution [3,5]. In addition, nerve dysfunction due to traction injury or compression [6,7] may be associated with tendon rupture. Suprascapular neuropathy has been implicated in 8%-100% of massive rotator cuff tears [7]. Experimental studies in rodents and sheep have shown that the ablation of neuronal input may counteract some degenerative processes, such as the reduction of fast-type muscle fibers [8,9] and infiltration [10], in the released skeletal muscle but exaggerate muscle atrophy [11] and increase fat content [9,12].

The molecular processes underlying muscle degeneration after tenotomy and denervation are not completely understood [13]. Altered expression of gene regulatory factors and gene transcripts, especially those involved in myogenic and adipogenic processes, may contribute to a better understanding of the cellular mechanisms underlying muscle structure changes after impact or the absence of physiological stimuli [9,12,14]. For example, combined neurectomy and tendon release transiently increased adipogenic and myogenic transcript expression at 2 and 8 weeks after surgery[9]. Thus, muscular adjustments after tenotomy or neurectomy involve sarcolemma-associated factors, such as laminin-2/merosin, which influence muscle activity-dependent remodeling of the fiber architecture [15,16]. In addition, tenotomy or neurectomy may affect molecular aspects of muscle degeneration and regeneration [8], such as

calcium/calmodulin dependent kinase II (CaMKII) [17] and tenascin-C [18]. These proteins are important for neurogenic reactions, such as the increase in fast-type muscle fibers [12,19,20].

We hypothesized that the specific molecular reactions associated with the degeneration of muscle fibers into fat and fiber type transformations are related to the preservation of fast-type muscle fibers. We also hypothesized that the exaggerated atrophy in tenotomized infraspinatus muscle is associated with the ablation of neuronal drive. We assessed the protein expression levels of factors associated with myogenesis in slow and fast-type muscle fibers (myogenin and myogenic differentiation factor [myoD]) [12,21], sarcolemmal reactions (laminin-2) [15,22], fat differentiation (isoforms 1 and 2 of transcription factor peroxisome proliferator-activated receptor gamma [PPARG]) [23], and denervation-induced muscle regeneration (tenascin-C and CaMKII) [17,18].

Materials and Methods

Animal Model

Study protocols were carried out according to Swiss laws on animal welfare and approved by the local federal authorities (No. 72/2013). Three intervention groups of 6 female Swiss alpine sheep (age 25 ± 4 months; Staffelegg, Küttigen (AG), Switzerland) each underwent one of the following surgeries on the right shoulder under anesthesia: infraspinatus tenotomy (TEN), suprascapular nerve transection (neurectomy; NEU), or combined tenotomy and neurectomy (TEN-NEU). Biopsies were collected from non-overlapping lateral areas of the operated infraspinatus muscle during surgery (pre) and 16 weeks later (post), biopsies were taken from the operated on and contralateral control muscle. These samples were used to characterize muscle composition and

determine the relative content of specific proteins by sodium dodecyl sulfate poly acrylamide gel electrophoresis (SDS-PAGE)/immunoblotting. Magnet resonance imaging (MRI) of the shoulder region was performed at the pre and post time points to assess infraspinatus muscle volume.

Surgery

All surgical procedures were performed via a 15-cm curved incision 2 cm caudal to the scapular spine as described previously [11]. Sheep in the TEN group underwent 16 weeks of tendon release by osteotomy of a small bone chip from the greater tuberosity using an oscillating saw. Sheep in the NEU group underwent 16 weeks of denervation by suprascapular nerve transection via electrocautery of the scapular spine distal to the innervation of the supraspinatus muscle. Sheep in the TEN-NEU group underwent both surgical procedures. In the end, the sheep were sacrificed.

MRI

Sheep were sedated under anesthesia and positioned to orient both scapular spines in the imaging plane before both shoulders were scanned using a 3-T system (Philips Ingenia 3T with dStream body coil Solution, Philips AG) and processed as described previously [3]. The 2-mm transverse sections were recorded perpendicular to the glenoid cavity using T1- and T2-weighted sequences and smDixon water and Dixon fat pulse sequences. The fat fraction at the level of the central tendon and volumes of both infraspinatus muscles were computed in transverse Dixon images using a publicly available DICOM viewer (OsiriX v.5.6 32-bit, © Pixmeo SARL).

Biopsy Handling

Muscle biopsies (~50 mg) were collected from the lateral areas of the belly region of the infraspinatus muscle using a 5-mm Bergstroem needle (Dixons Surgical Instruments LTD, Wickford, UK), rapidly frozen in nitrogen-cooled isopentane, and kept individually in sealed 2-ml cryotubes (Greiner, Frickenhausen, Germany) at -80°C. Biopsy locations were marked with non-absorbable 3-0 sutures to avoid resampling a previously manipulated area.

Consecutive sections were prepared for subsequent analysis in a cryostat perpendicular to the major axis of muscle fibers. For the characterization of protein content, 25-µm-thick cryosections corresponding to a volume of ~10 mm^3 were pooled and frozen in a 2-ml tube at -80°C (Vaudaux-Eppendorf AG, Schönenbuch, Switzerland). For the characterization of muscle composition, pairs of 12-µm-thick cryosections were prepared from the middle portion of each biopsy and both samples from one sheep were mounted on microscopic slides (Superfrost®Plus, Menzel GmbH, Braunschweig, Germany), air-dried for 30-60 min at room temperature, and frozen at -80°C until used.

Characterization of Muscle Composition

Consecutive 12-µm-thick sections from frozen muscle biopsies were prepared in a cryostat (Leica CM3050S, Leica Biosystems, Muttenz, Switzerland). Biopsies were oriented to section most fiber profiles perpendicular to the major fiber axis. Consecutive sections were stored at -80°C until processing by one of three methods: the Goldner trichrome method, Red Oil O staining, or immunofluorescent double staining for slow and fast myosin heavy chains [3,24](Fig. 2-S2). On the stained sections, microscopic fields were digitally recorded using an IX50 microscope with a digital camera DP72 (Olympus Schweiz AG) operating with Cell Sens Dimension software (Version 1.6, Olympus

Corporation). Images were exported as TIFF files in Adobe Photoshop CC (Adobe Systems Incorporated) to identify the area percentage of muscle cross sections covered by slow- and fast-type muscle fibers, connective tissue, and lipids using manual-directed identification of the stained areas with the lasso tool. Areas where fiber profiles were sectioned in a longitudinal fashion (i.e., with a circularity <0.6) were excluded from the analysis. Numbers from the different fields were summed for the cellular structures to calculate the respective percentages for the entire cross section/biopsy. The percentage of extracellular ground substance of the connective tissue was calculated as the difference between the area percentage of lipids and area percentage of connective tissue.

Protein Detection

Total homogenates were prepared and proteins were separated on 7.5% SDS-PAGE gels. Each lane contained 20 µg of denatured total protein. Each gel included both samples from one sheep for each of the three interventions in adjacent lanes. Proteins of interest were detected by immunoblotting with specific antibodies based on enhanced chemiluminescence as described previously [25,26]. The following primary antibodies were used: Tenascin-C antibody B28.13 (gift from Prof. R. Chiquet-Ehrismann), laminin antibody (PA1-32130, Thermo Fisher, Life Technologies Europe B.V., Zug, Switzerland) recognizing the α2 (150 kDa) and β1/γ1 (200 kDa) subunits [27,28], PPARG antibody (LS-C178333, Lifespan Biosciences Inc., LabForce AG, Nunningen, Switzerland), myogenin antibody F5D (SC-12732, Santa Cruz Biotechnology, LabForce AG, Nunningen, Switzerland), myoD antibody (SC-304, Santa Cruz Biotechnology, LabForce AG, Nunningen, Switzerland), CaMKII antibody (#611293, BD Biosciences, Allschwil, Switzerland), and skeletal alpha actin (A-2172, Sigma, Buchs, Switzerland). Horseradish

peroxidase-conjugated goat anti-rabbit (#55676, MP Biomedicals, Zurich, Switzerland) or goat anti-mouse (#9917, Sigma, Buchs, Switzerland) secondary antibodies were used. Tenascin-C, PPARG (Fig. S3), and myogenin were detected on the same blot after separating the respective areas using scissors. The laminin isoforms and myoD were detected on the same blot, but CaMKII was analyzed separately. For the detection of skeletal alpha actin, membranes were stripped before antibody incubation. The efficiency of protein loading was visualized by Ponceau S staining. The band intensity of the tagged protein was background-corrected and related to the band intensity of sarcomeric actin.

Protein Localization

Paraformaldehyde-fixed and goat serum-absorbed muscle sections were double-stained by incubation with fast-type myosin antibody (#M4276, Sigma, Buchs, Switzerland or #ab91506 Abcam, Cambridge, United Kingdom) and an antibody against CaMKII (#611293, BD Biosciences, Allschwil, Switzerland), myoD (SC-304, Santa Cruz Biotechnology, LabForce AG, Nunningen, Switzerland), or tenascin-C (#473, gift Prof. Matthias Chiquet) [29], followed by a mix of Alexa Fluor 555-coupled anti-mouse and Alexa Fluor 488-coupled goat anti-rabbit antibody (#A21425 and #A11017, Life Technologies) as described previously [30,11]. Nuclei were counter-stained with Hoechst 33342 (#62249, Thermo Scientific). Immunofluorescent images were recorded from non-overlapping microscopic fields on the excited sections for the red, green, and blue channels using a fluorescent microscope (Olympus IX50) with a DP72 digital camera operated by Cell Sens Dimension software (version 1.6, Olympus, Volketswil, Switzerland). The different channels of the recorded images were assembled using image J (http://rsbweb.nih.gov/ij/). Fibers in the phase contrast image that did not stain

for fast-type myosin were classified as slow-type muscle fibers. The association of the detected protein with muscle fibers was assessed by counting single- or double-positive fast and (unstained) slow-type fibers after processing the images with Image J. Counting was done in a dark environment on a 24-inch 1920x1080 60Hz LED Monitor (ACER, LG Electronics). A transparency with a grid of squares (10.65 x 10.65 cm) was laid on the monitor to manually count and mark stained muscle fibers. On average, 541 fibers were counted per section. The observer error for assessing the associations between CaMKII and slow and fast-type muscle fibers was below 2%.

Statistical Analysis

All statistical analyses were performed using SPSS (version 22, IBM corporation) or MS-Excel (Kildare, Ireland). Values are presented as mean ± standard error (SE). The actin-related expression levels of the detected proteins were normalized to the mean values of the pre-samples for the six respective immunoblots, pooled, and the resulting values were related to the median pre-values for the respective intervention to determine the relative expression levels per contractile material [31]. Effects of time and intervention were analyzed by a repeated ANOVA for the factor "intervention group" (TEN, NEU, TEN-NEU) and repeated factor "time-point" (pre, post). Effects were localized using a Fisher's post-hoc test. Differences were significant if $p < 0.05$. Interrelationships between the 6 cellular and 10 molecular parameters were calculated based on a Pearson correlation analysis of the measures from all 36 (biopsy) sample points and considered significant if they passed Bonferroni-corrected p-values of 0.05, calculated by dividing the estimated p-value by the number of unique comparisons. Chi-squared was used to identify whether an association effect existed between fiber type and the localization of the protein of interest (CaMKII, myoD). G-tests were then used to localize the effect.

Results

Animals

The body mass increased for the intervention groups undergoing tenotomy when comparing the values at surgery and 16 weeks post-surgery (45.3 ± 1.8 vs. 55.7 ± 1.8 kg, $p<0.001$ for the TEN group and 55.5 ± 1.9 vs. 60.0 ± 1.9 kg, $p<0.001$ for the TEN-NEU group). In the NEU group the corresponding values were 56.3 ± 1.5 vs. 60.7 ± 2.3 kg ($p=0.115$).

Muscle Anatomy

The volume of the infraspinatus muscle decreased from 166 ± 6 to 130 ± 8 cm^3 in the TEN group. Compared with this change of -22 ± 8%, the infraspinatus volume decreased more in the NEU (-53 ± 8%) and TEN-NEU groups (-51 ± 16%; Fig. 1). Sixteen weeks after the intervention, the fat fraction in the central region of the infraspinatus muscle was increased in the TEN group (from 12% to 50%), TEN-NEU group (13% to 46%), and NEU group (13% to 40%).

Muscle Composition

In the biopsy samples, the area percentage of connective tissue increased similarly in all intervention groups after 16 weeks with a concurrent loss in contractile tissue (Fig. 2). The area percentage of extracellular ground substance also increased after all three interventions: to 32% (+387%) in the NEU group, 33% (+389%) in the TEN-NEU group, and 41% (+457%) in the TEN group (Fig. 3A). In the TEN group, the area percentage of lipids increased to 31% (+292%), but this parameter was not affected in the NEU ($p= 0.35$) or TEN-NEU groups ($p=0.16$, Fig. 3B). In the two NEU groups, cells were identified

that were defined by a basal lamina but did not contain cytoplasmic material or stain for lipids (Fig. 3C,D). In the TEN group, the area percentage of fast-type muscle fibers decreased by 26% (Fig. 4). In the NEU and TEN-NEU groups, the area percentage of slow-type muscle fibers decreased by 7% and 18%, respectively. The area percentage of hybrid slow-/fast-type fibers increased in the NEU and TEN-NEU groups, but not the TEN group (Fig. 4).

Protein Expression

The targeted proteins were detected in all samples (Fig. 5). Intervention-specific upregulation was measured 16 weeks after surgery (Fig. 6). There was an interaction effect between the 'intervention group' and 'time-point' ($p=0.016$) that was explained by the larger effect of combined neurectomy and tenotomy on protein expression. The expression of myoD increased in denervated muscle (NEU: +217%, NEU-TEN: +242%); whereas, the levels of the beta M isoform of CaMKII (βMCaMKII) increased in the tenotomy groups (TEN: +124%, NEU-TEN: +112%). The levels of the delta isoform of CaMKII (δCaMKII) and isoforms 1 and 2 of the adipocyte differentiation marker PPARG increased only in the TEN-NEU group (+119%, +84%, and +81%, respectively). The relative abundances of the CaMKII isoforms were 23% (βMCaMKII), 47% (δCaMKII), and 30% (γCaMKII). The level of α2 laminin increased in the TEN (+40%) group.

Protein Localization

The localization of the myoD and CaMKII proteins demonstrated intervention-specific regulation. MyoD was detected in nuclei and associated with muscle fibers (Fig. S4). CaMKII was detected close to the sarcolemma and strong immune-reactive sarcoplasma within certain muscle fibers (Fig. S4). Sixteen weeks after neurectomy (NEU or TEN-

NEU), nuclear myoD staining was more frequently associated with slow-type muscle fibers than fast-type (18% and 12%, respectively); while, sarcoplasmic CaMKII staining was more abundant in slow muscle fibers than fast-types (25% and 12%, respectively).

Interrelationships

Correlations between and within molecular and cellular parameters are provided in Tables S1 and S2. The most inter-connected parameter was the area density of muscle fibers and volume of the infraspinatus muscle. Parameters that greatly contributed to the characteristics of normal muscle (i.e., the area percentage of muscle fibers and muscle volume) negatively correlated with the characteristics of muscle degeneration (i.e., the area percentage of lipid and extracellular ground substance; Table S1). The fat fraction more strongly correlated with the area percentages of connective tissue and extracellular ground substance than the area percentage of lipids. Conversely, the area percentage of muscle fibers positively correlated with the area percentage of slow- and fast-type muscle fibers and muscle volume (Table S1). Muscle volume and the area percentage of muscle fibers negatively correlated with the expression of βMCaMKII (Table S1). Conversely, the area percentage of extracellular ground substance positively correlated with PPARG1, myoD, and δ and γCaMKII. All interrelated protein levels had positive correlations (Table S2).

Discussion

The skeletal muscle phenotype is brought about by use-related mechanical and metabolic cues during nerve-evoked contractions [12,32]. Here, ablation of neuronal input to the infraspinatus muscle in sheep produced a specific pattern of cellular alterations, including changes in the area percentage of muscle fibers and extracellular ground substance, muscle volume, and the levels of the myogenic transcription factor myoD. Notably, increases in protein levels were generally higher when neurectomy was combined with tenotomy, but this did not manifest at the level of muscle composition. However, tenotomy induced a specific increase in sarcoplasmic reticulum-associated βMCaMKII; although, it did not affect expression of tenascin-C, a denervation-associated extracellular matrix (ECM) protein [16,18].

The group-specific changes in the expression of the βM and δ CaMKII isoforms, especially the "subtractive" effect of denervation on βCaMKII levels and the additive effect on δCaMKII levels, are consistent with the reported expression of CaMKII isoforms 14 days after denervation in mouse plantaris muscle [33]. All CaMKII isoform levels positively correlated with the area percentage of hybrid fibers, indicating muscle degeneration [34]. The level of βMCaMKII, which regulates the sarcoplasmic calcium pump [20], also correlated with muscle volume and the area percentage of fast muscle fibers (Table S1), but not slow muscle fibers (P=0.15). In models of muscle plasticity, it was implied that CaMKII protein levels reflect the calcium-inducible CaMKII activity [35,36]. Therefore, our findings indicate that alterations in the fiber-type and muscle volume after neurectomy and/or tenotomy are reflected by an increased capacity for calcium-regulated signaling/handling by distinct CaMKII isoforms, as reviewed by Eilers et al [37].

The CaMKII isoforms are possible mediators of the calcium-regulated fiber type transformations [38,37]. In particular, δCaMKII isoforms are associated with the regulation of gene expression [37] and demonstrate muscle-type specific expression, which is modified by denervation in chickens and mice [17,20,33]. The δCaMKII protein was the most abundant CaMKII isoform in the present study (Fig. 5). The elevated immunofluorescence for CaMKII in the sarcoplasm of slow-type muscle fibers (Fig. S4) is consistent with the localization of δCaMKII protein [39] and the enhanced δCaMKII expression in the sarcoplasm of regenerating muscle fibers [39]. Collectively, our findings indicate that enhanced δCaMKII levels contribute to the activation of a fast-contractile gene program in tenotomized and denervated infraspinatus muscle.

Histological analysis demonstrated that the increased area percentage of connective tissue in the lateral muscle region of sheep in the two neurectomy groups was explained by an increased area percentage of extracellular ground substance and not by alterations in the area percentage of lipids (compare Fig. 3A and 3B). These microscopic findings contrast previous MRI- and CT-based measurements of the fat fraction, showing that fatty infiltration in the central tendon region of the infraspinatus muscle increased from 13% to 40% in the NEU group 16 weeks after surgery [11]. Notably, the fat fraction in the central tendon portion of the studied bi-pennate muscle correlated better with the area percentage of extracellular ground substance than lipids in the biopsy sample ($r=0.88$ vs. 0.50; Table S1). Disconnected reactions between the extracellular ground substance and lipid processes are supported by qualitative observations in the biopsies from the NEU group, showing that cells with a size and boundary corresponding to muscle fibers did not demonstrate cytoplasmic staining with Goldner trichrome or Red-Oil. This observation is in line with previous publications on the effect of denervation on the soleus muscle in rats [40]. We identified a correlation between the area percentage of

extracellular ground substance and the total concentration of PPARG1 and 2 [41,42], as they were up-regulated in the TEN-NEU group. Thus, the combination of neurectomy and tenotomy increases the capacity for adipogenesis in a manner that may not be confined to fat cells, and could include adipogenic progenitors in the interstitium [43,44].

The increased levels of α2 laminin in the TEN group are in line with the increased expression of ECM proteins after tendon rupture [45]. Expression of tenascin-C, which is associated with muscle fiber and nerve regeneration in denervated muscle [16,18], was not significantly affected 16 weeks after surgery in the intervention groups. However, tenascin-C protein levels correlated with α2 and β1γ1 laminin levels, the area percentage of extracellular ground substance, and the myogenic transcription factors myoD, myogenin, and PPARG1/2. These observations are consistent with myogenesis and connective tissue reactions being coordinated by a process involving tenascin-C in damaged muscle [25], but do not support major alterations in muscle regeneration 16 weeks after tendon release.

Regarding myogenesis, there were interesting correlations between the levels of the myogenic regulators myoD and δ/γCaMKII and denervation-specific effects on the area percentage of extracellular ground substance and muscle fibers, and muscle volume. Elevated levels of CaMKII isoforms and myoD were associated with increased fast-type myosin heavy chain expression during muscle regeneration [25,37]. We identified associations between nuclear myoD and sarcoplasmic CaMKII and slow-type muscle fibers in the TEN-NEU group 16 weeks after surgery. Thus, increased expression of myoD, and possibly δCaMKII, reflect a fast-contractile gene program induced by neurectomy in slow-type muscle fibers. These molecular reactions may help us to better understand the mechanism through which nerve transection preserves the area percentage of fast-type muscle fibers in the released infraspinatus muscle (Fig. S5).

Our study has some limitations. First, biopsy samples were collected from a single site per muscle and time point. It could be argued that this is not representative of alterations over the entire muscle due to regional anatomical differences [46]. We also noted a difference in the type I/II fiber composition at the pre-sample point in the TEN group compared with the NEU and TEN-NEU groups. Differences between the more abundant slow and fast-type fibers were not significant at the pre-sample point, suggesting that these did not affect the identified effects of the interventions on fiber type distribution and molecular markers.

In conclusion, our molecular observations in sheep suggest nerve injury makes a minor contribution to the pathological remodeling of muscle after experimental release of the rotator cuff muscle. Furthermore, our findings support that transection of the suprascapular nerve offsets, at least in part, adjustments in muscle quality after tendon release. These reactions are not complete 16 weeks after surgery. Elevated expression of myoD and CaMKII in slow fiber-associated nuclei and sarcoplasm, respectively, indicates that neurectomy activates a fast-contractile gene program that mitigates the loss in the area percentage of fast muscle fibers but does not prevent the removal of contractile material.

Abbreviations

ANOVA: Analysis of variance

α2laminin: alpha 2 isoform of laminin

β1γ1 laminin: beta 1 / gamma 1 isoform of laminin

βMCaMKII: beta M isoform of CaMKII

CaMKII: calcium/calmodulin dependent kinase II

CT: computed tomography

ECM: extracellular matrix

δCaMKII: delta isoform of CaMKII

γCaMKII: gamma isoform of CaMKII

MRI: magnetic resonance imaging

myoD: myogenic differentiation factor

NEU: neurectomy

PPARG: peroxisome proliferator-activated receptor gamma

SDS-PAGE: sodium dodecyl sulfate poly acrylamide gel electrophoresis

TEN: tenotomy

TEN-NEU: combined tenotomy and neurectomy

References

1. Yamaguchi K, Ditsios K, Middleton WD, Hildebolt CF, Galatz LM, Teefey SA. The demographic and morphological features of rotator cuff disease. A comparison of asymptomatic and symptomatic shoulders. *J Bone Joint Surg Am* 2006;**88**:1699-1704.
2. Minns Lowe CJ, Moser J, Barker K. Living with a symptomatic rotator cuff tear 'bad days, bad nights': a qualitative study. *BMC Musculoskelet Disord* 2014;**15**:228.
3. Gerber C, Meyer DC, Fluck M, Benn MC, von Rechenberg B, Wieser K. Anabolic Steroids Reduce Muscle Degeneration Associated With Rotator Cuff Tendon Release in Sheep. *Am J Sports Med* 2015;**43(10)**:2393-2400.
4. Laron D, Samagh SP, Liu X, Kim HT, Feeley BT. Muscle degeneration in rotator cuff tears. J Shoulder Elbow Surg 2012;**21(2)**:164-174.
5. Gumucio JP, Davis ME, Bradley JR, Stafford PL, Schiffman CJ, Lynch EB, Claflin DR, Bedi A, Mendias CL. Rotator cuff tear reduces muscle fiber specific force production and induces macrophage accumulation and autophagy. *J Orthop Res* 2012;**30(12)**:1963-1970.
6. Yanny S, Toms AP. MR patterns of denervation around the shoulder. *AJR Am J Roentgenol* 2010;**195(2)**:W157-163.
7. Shi LL, Freehill MT, Yannopoulos P, Warner JJ. Suprascapular nerve: is it important in cuff pathology? *Adv Orthop* 2012;**2012**:516985.
8. Tews DS, Goebel HH, Schneider I, Gunkel A, Stennert E, Neiss WF. Morphology of experimentally denervated and reinnervated rat facial muscle. I. Histochemical and histological findings. *Eur Arch Otorhinolaryngol* 1994;**251(1)**:36-40.

9. Kim HM, Galatz LM, Lim C, Havlioglu N, Thomopoulos S. The effect of tear size and nerve injury on rotator cuff muscle fatty degeneration in a rodent animal model. *J Shoulder Elbow Surg* 2012;**21(7)**:847-858.

10. McMinn RM, Vrbova G. The Effect of Tenotomy on the Structure of Fast and Slow Muscle in the Rabbit. *Q J Exp Physiol Cogn Med Sci* 1964;**49**:424-429.

11. Gerber C, Meyer DC, Fluck M, Valdivieso P, von Rechenberg B, Benn MC, Wieser K. Muscle Degeneration Associated With Rotator Cuff Tendon Release and/or Denervation in Sheep. *Am J Sports Med* 2017;**45(3)**:651-658.

12. Fluck M, Hoppeler H. Molecular basis of skeletal muscle plasticity--from gene to form and function. *Rev Physiol Biochem Pharmacol* 2003;**146**:159-216.

13. Wang Y, Pessin JE. Mechanisms for fiber-type specificity of skeletal muscle atrophy. *Curr Opin Clin Nutr Metab Care* 2013;**16(3)**:243-250.

14. Phillips K. PHENOTYPIC PLASTICITY. Journal of Experimental Biology 2009; **209**: (i-iii).

15. Bezakova G, Lomo T. Muscle activity and muscle agrin regulate the organization of cytoskeletal proteins and attached acetylcholine receptor (AchR) aggregates in skeletal muscle fibers. *J Cell Biol* 2001;**153**(7):1453-1463.

16. Sanes JR, Apel ED, Burgess RW, Emerson RB, Feng G, Gautam M, Glass D, Grady RM, Krejci E, Lichtman JW, Lu JT, Massoulie J, Miner JH, Moscoso LM, Nguyen Q, Nichol M, Noakes PG, Patton BL, Son YJ, Yancopoulos GD, Zhou H. Development of the neuromuscular junction: genetic analysis in mice. *J Physiol Paris* 1998;**92(3-4)**:167-172.

17. Wang X, Rostas JA. Protein phosphorylation in fast and slow chicken skeletal muscles: effect of denervation. Muscle Nerve 1998;**21(4)**:504-513.

18. Schoser BG, Goebel HH. Tenascin in denervated human muscle. *J Neurol Sci* 1996;139(2):203-209.

19. Tosi C, Jerusalem F. [Selective muscle fiber type anomalies in neuromusclar disorders. An analysis of 124 consecutive muscle biopsies (author's transl)]. *J Neurol* 1976;**214(1)**:13-34.

20. Eilers W, Gevers W, van Overbeek D, de Haan A, Jaspers RT, Hilbers PA, van Riel N, Fluck M. Muscle-type specific autophosphorylation of CaMKII isoforms after paced contractions. *Biomed Res Int* 2014;**2014**:943806.

21. Hughes SM, Koishi K, Rudnicki M, Maggs AM. MyoD protein is differentially accumulated in fast and slow skeletal muscle fibres and required for normal fibre type balance in rodents. *Mech Dev* 1997;**61(1-2)**:151-163.

22. Patton BL, Connoll AM, Martin PT, Cunningham JM, Mehta S, Pestronk A, Miner JH, Sanes JR. Distribution of ten laminin chains in dystrophic and regenerating muscles. *Neuromuscul Disord* 1999;**9(6-7)**:423-433.

23. Floyd ZE, Stephens JM. Controlling a master switch of adipocyte development and insulin sensitivity: covalent modifications of PPARgamma. *Biochim Biophys Acta* 2012;**1822(7)**:1090-1095.

24. Goldner J. A modification of the masson trichrome technique for routine laboratory purposes. Am J Pathol 1938;**14(2)**:237-243.

25. Fluck M, Mund SI, Schittny JC, Klossner S, Durieux AC, Giraud MN. Mechano-regulated tenascin-C orchestrates muscle repair. *Proc Natl Acad Sci U S A* 2008;**105(36)**:13662-13667.

26. Fluck M, Ruoss S, Mohl CB, Valdivieso P, Benn MC, von Rechenberg B, Laczko E, Hu J, Wieser K, Meyer DC, Gerber C. Genomic and lipidomic actions of nandrolone

on detached rotator cuff muscle in sheep. *J Steroid Biochem Mol Biol* 2017;**165(Pt B)**:382-395.

27. Herrera C, Macedo JK, Feoli A, Escalante T, Rucavado A, Gutierrez JM, Fox JW. Muscle Tissue Damage Induced by the Venom of Bothrops asper: Identification of Early and Late Pathological Events through Proteomic Analysis. *PLoS Negl Trop Dis* 2016;**10(4)**:e0004599.
28. Schuler F, Sorokin LM. Expression of laminin isoforms in mouse myogenic cells in vitro and in vivo. J Cell Sci 1995;**108 (Pt 12)**:3795-3805.
29. Fluck M, Tunc-Civelek V, Chiquet M. Rapid and reciprocal regulation of tenascin-C and tenascin-Y expression by loading of skeletal muscle. *J Cell Sci* 2000;**113 (Pt 20)**:3583-3591.
30. Ruoss S, Mohl CB, Benn MC, von Rechenberg B, Wieser K, Meyer DC, Gerber C, Fluck M. Costamere protein expression and tissue composition of rotator cuff muscle after tendon release in sheep. *J Orthop Res* 2018; **36(1)**:272-281.
31. Borina E, Pellegrino MA, D'Antona G, Bottinelli R. Myosin and actin content of human skeletal muscle fibers following 35 days bed rest. *Scand J Med Sci Sports* 2010;**20(1)**:65-73.
32. Booth FW, Thomason DB. Molecular and cellular adaptation of muscle in response to exercise: perspectives of various models. *Physiol Rev* 1991;**71(2)**:541-585.
33. Williams B. CaMKII Protein Expression and Phosphorylation in Mouse Skeletal Muscle Following Atrophy and Hypertrophy. Greenville: East Carolina University; 2012.
34. Minamoto V, Shlvini T. LONG-TERM REGENERATION OF RAT SKELETAL MUSCLE AFTER PERIODIC CONTUSIONS. *Rev bras fisioter* 2002;**6(3)**:147-154.

35. Fluck M, Waxham MN, Hamilton MT, Booth FW. Skeletal muscle Ca(2+)-independent kinase activity increases during either hypertrophy or running. *J Appl Physiol* (1985) 2000;**88(1)**:352-358.

36. Fluck M, Booth FW, Waxham MN. Skeletal muscle CaMKII enriches in nuclei and phosphorylates myogenic factor SRF at multiple sites. *Biochem Biophys Res Commun* 2000;**270(2)**:488-494.

37. Eilers W, Jaspers RT, de Haan A, Ferrie C, Valdivieso P, Fluck M. CaMKII content affects contractile, but not mitochondrial, characteristics in regenerating skeletal muscle. *BMC Physiol* 2014;**14**:7.

38. Lopez JR, Allen P, Alamo L, Ryan JF, Jones DE, Sreter F. Dantrolene prevents the malignant hyperthermic syndrome by reducing free intracellular calcium concentration in skeletal muscle of susceptible swine. *Cell Calcium* 1987;**8(5)**:385-396.

39. Abraham ST, Shaw C. Increased expression of deltaCaMKII isoforms in skeletal muscle regeneration: Implications in dystrophic muscle disease. *J Cell Biochem* 2006;**97(3)**:621-632.

40. Vrbova G. Changes in the motor reflexes produced by tenotomy. *J Physiol* 1963;**166**:241-250.

41. Schoonjans K, Staels B, Auwerx J. Role of the peroxisome proliferator-activated receptor (PPAR) in mediating the effects of fibrates and fatty acids on gene expression. *J Lipid Res* 1996;**37(5)**:907-925.

42. Vidal-Puig AJ, Considine RV, Jimenez-Linan M, Werman A, Pories WJ, Caro JF, Flier JS. Peroxisome proliferator-activated receptor gene expression in human tissues. Effects of obesity, weight loss, and regulation by insulin and glucocorticoids. *J Clin Invest* 1997;**99(10)**:2416-2422.

43. Langevin HM, Nedergaard M, Howe AK. Cellular control of connective tissue matrix tension. J Cell Biochem 2013;114(8):1714-1719.

44. Hamrick MW, McGee-Lawrence ME, Frechette DM. Fatty Infiltration of Skeletal Muscle: Mechanisms and Comparisons with Bone Marrow Adiposity. *Front Endocrinol (Lausanne)* 2016;**7**:69.

45. Karousou E, Ronga M, Vigetti D, Passi A, Maffulli N. Collagens, proteoglycans, MMP-2, MMP-9 and TIMPs in human achilles tendon rupture. *Clin Orthop Relat Res* 2008;**466(7)**:1577-1582.

46. Suzuki A. Differences in distribution of myofiber types between the supraspinatus and infraspinatus muscles of sheep. *Anat Rec* 1995;**242(4)**:483-490.

Figure legends

Figure 1: ***Alterations in muscle volume.*** Data are presented as the median + standard error (box and central line) and minima/maxima (whisker) of the percent difference in infraspinatus muscle volume at 16 weeks post-surgery vs. pre-values in the three intervention groups that underwent tenotomy (TEN), neurectomy (NEU), or combined tenotomy and neurectomy (TEN-NEU). †p<0.05 vs. TEN.

Figure 1

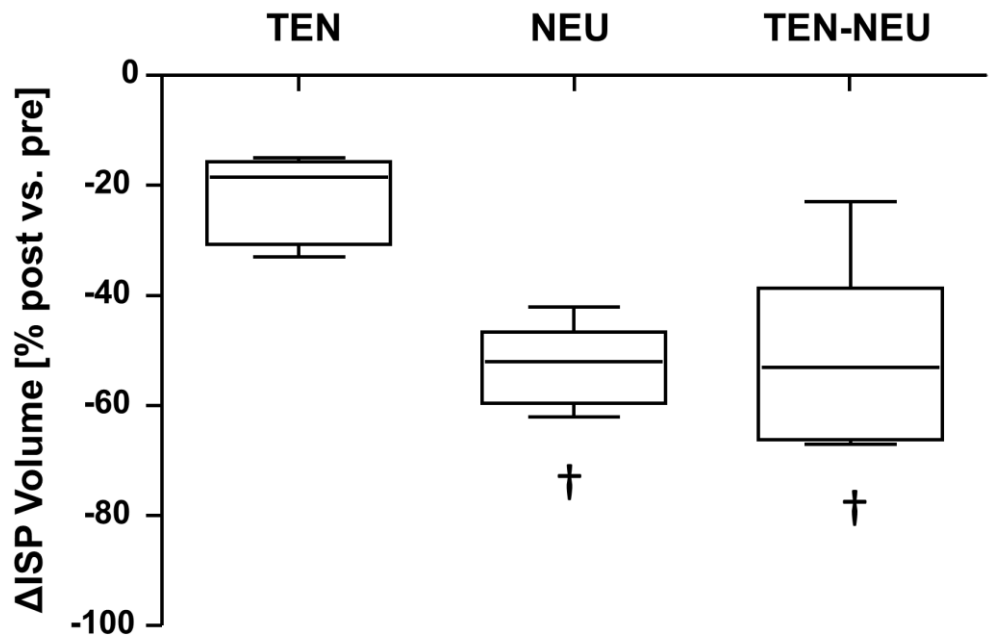

Figure 2: ***Changes in connective tissue and contractile tissue.*** Stapled bar graph of the mean + standard error for the area percentages of connective and contractile tissue pre- and post-surgery for the three intervention groups that underwent tenotomy (TEN),

neurectomy (NEU), or combined tenotomy and neurectomy (TEN-NEU). * denotes p<0.05 vs. pre (ANOVA with post-hoc test of Fisher). N=6 per group.

Figure 2

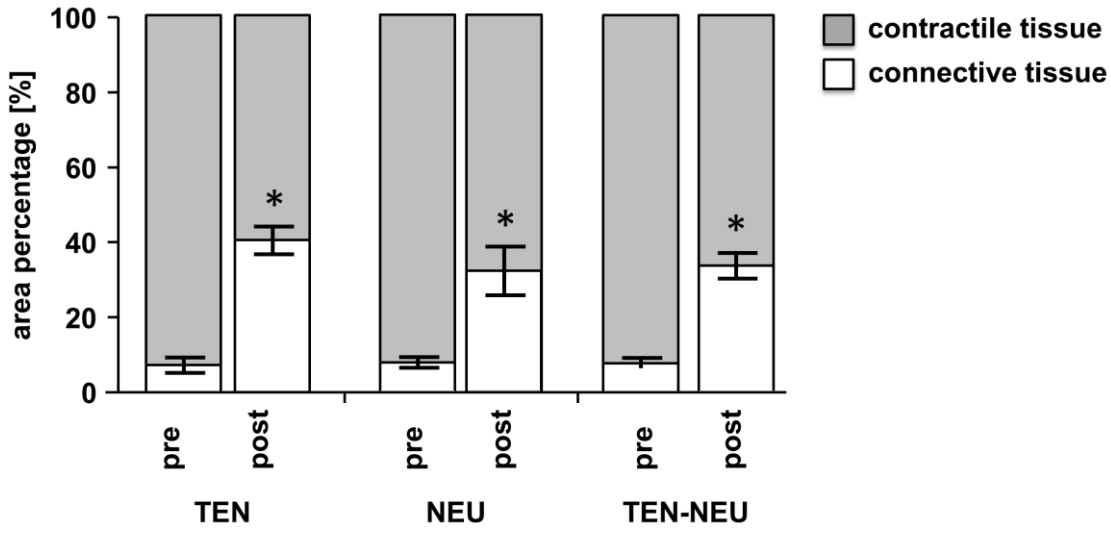

Figure 3: ***Alterations in lipid and extracellular matrix compositions.*** (A) The median + standard error (box and central line) and minima/maxima (whisker) difference in the area percentage per total cross section for extracellular ground substance (ECM) and (B) lipids in the connective tissue of the infraspinatus muscle before (pre) and 16 weeks after (post) surgery in the three intervention groups that underwent tenotomy (TEN), neurectomy (NEU), or combined tenotomy and neurectomy (TEN-NEU). (C) Microscopic fields of Red Oil O and (D) Goldner-stained consecutive sections in the TEN-NEU group 16 weeks after the intervention. Black arrows indicate the region corresponding to the red stained lipids. The thick green arrow indicates the green-stained ECM. Thin green arrows indicate circular structures, which are defined by a red basal lamina cylinder in (D), but do not demonstrate red cytoplasmic Goldner trichrome staining. *p<0.05 vs. pre (ANOVA with post-hoc Fisher test). N=6 per group. †p<0.05 vs. TEN.

Figure 3

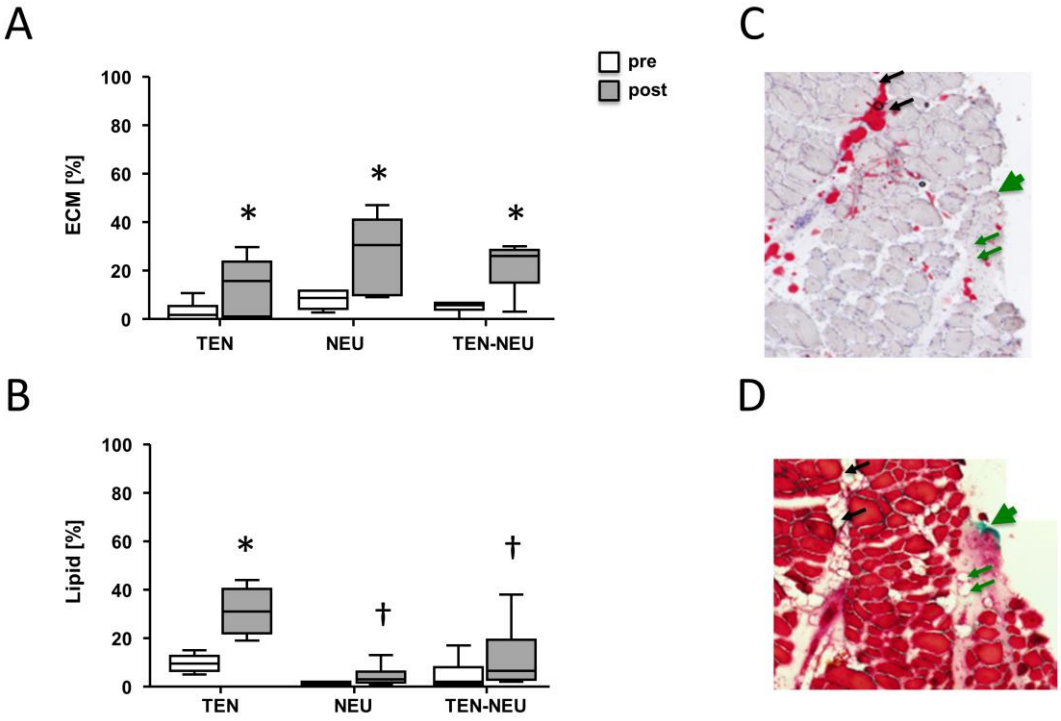

Figure 4: ***Alterations in muscle fiber composition.*** Area percentages of slow-type, fast-type, and hybrid type muscle fibers from infraspinatus muscle per contractile tissue at 16 weeks post-surgery vs. pre-values in the three intervention groups that underwent tenotomy (TEN), neurectomy (NEU), or combined tenotomy and neurectomy (TEN-NEU). N=6 per group. *p<0.05 vs. pre. †p<0.05 vs. TEN.

Figure 4

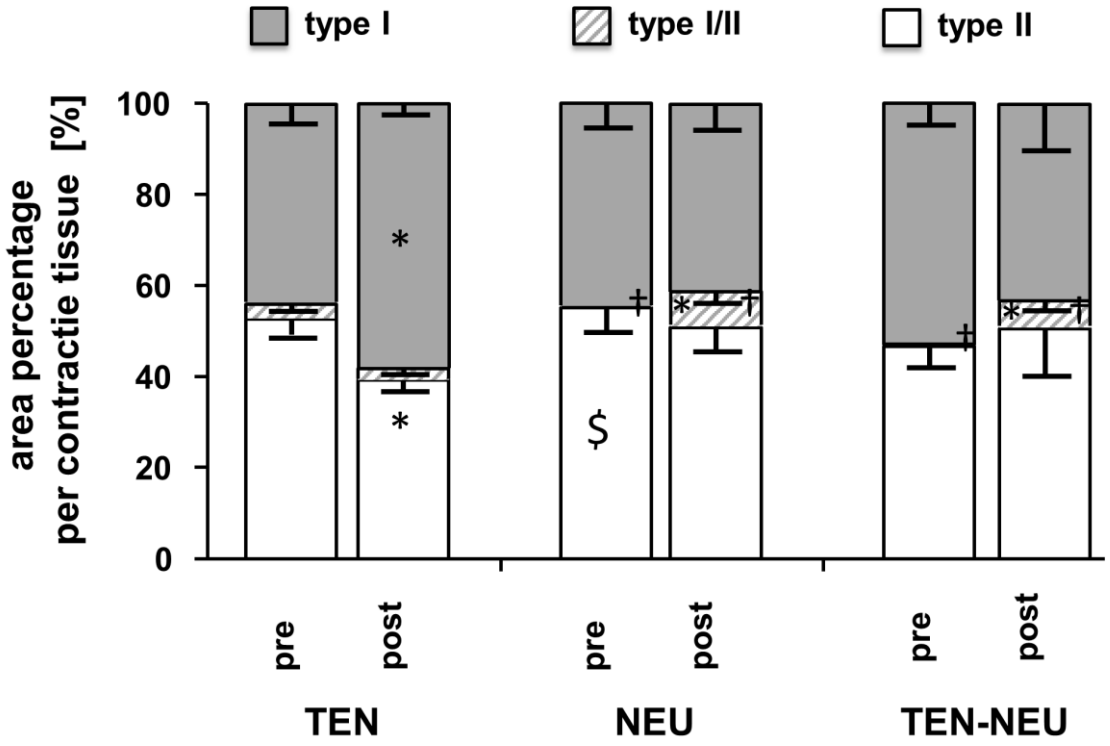

Figure 5: ***Protein detection.*** Example immunoblots visualizing the assessed markers of denervation-induced muscle regeneration (A, tenascin-C; B, βM, δ, and γCaMKII), fat cell differentiation (C, PPARG1/2), sarcolemmal remodeling (D, α2, and β1γ1 laminin), and myogenesis (E, myogenin; F, myoD) in pre- and post- surgery samples of infraspinatus muscle for all three intervention groups that underwent tenotomy (TEN), neurectomy (NEU), or combined tenotomy and neurectomy (TEN-NEU). The internal reference sarcomeric actin is shown below the blots. The names and sizes (in kilodaltons, kDa) of the protein bands of interest are noted on the right and left, respectively.

Figure 5

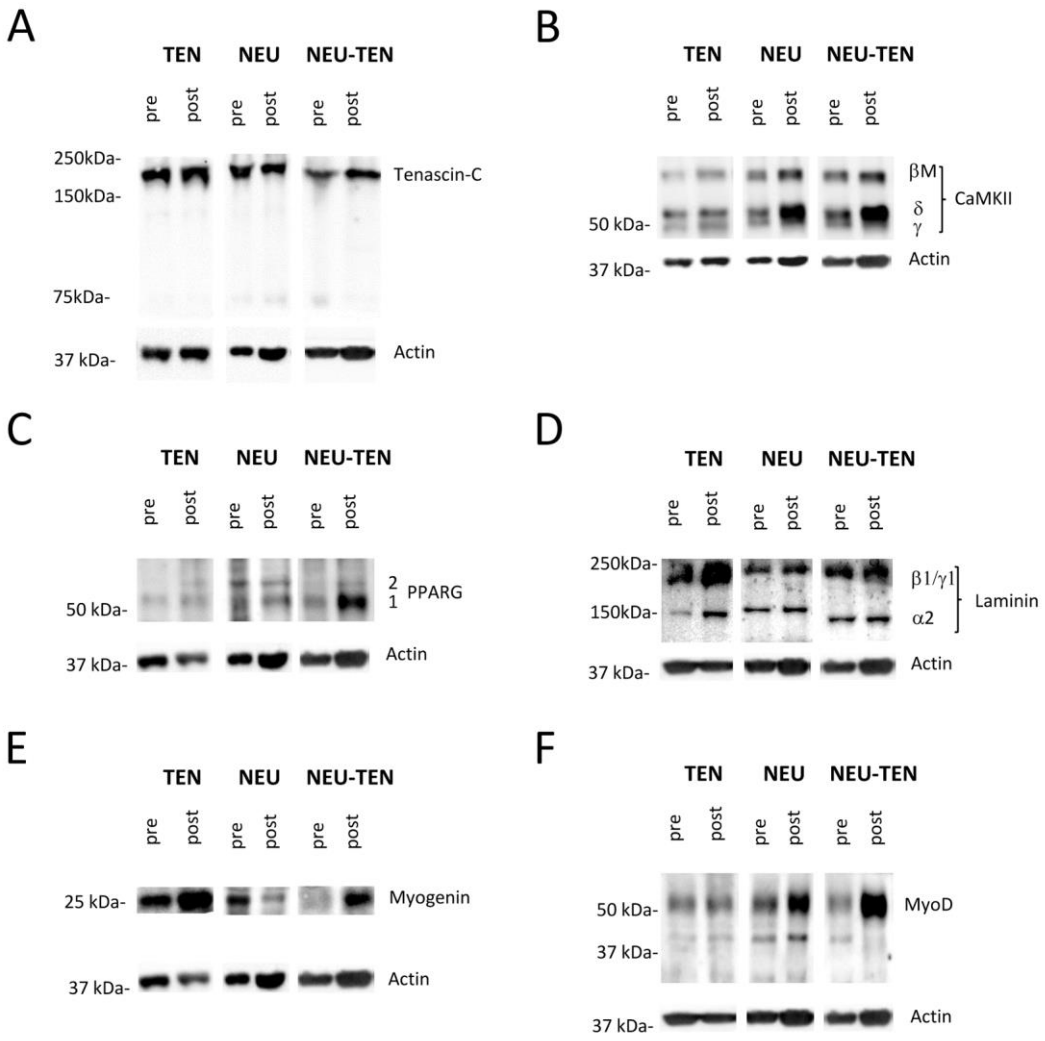

Figure 6: ***Changes in protein levels.*** Data are presented as the mean + standard error for the expression levels of the assessed proteins relative to skeletal alpha actin. A-C) Expression values for the proteins pre- and 16 weeks post-surgery in the groups that underwent tenotomy (A), neurectomy (B), or combined tenotomy and neurectomy (C). N=6 per group. *p<0.05 vs. pre. †p<0.05 vs. TEN. Note the larger effect of the combination of tenotomy and neurectomy on protein expression levels in the post-surgical samples.

Figure 6